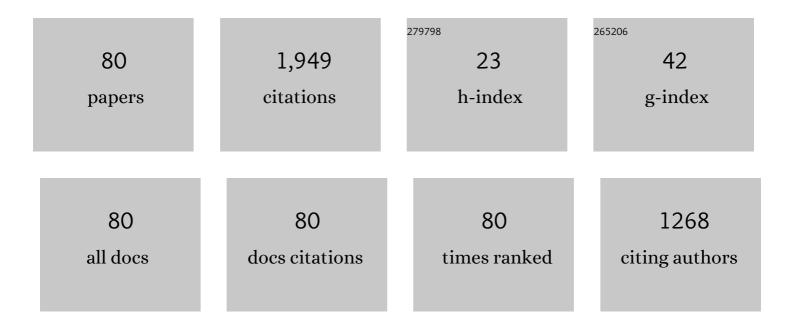
List of Publications by Year in descending order

Source: https://exaly.com/author-pdf/9603135/publications.pdf Version: 2024-02-01



#	Article	IF	CITATIONS
1	A higher-than-predicted measurement of iron opacity at solar interior temperatures. Nature, 2015, 517, 56-59.	27.8	321
2	Isochoric Heating of Solid Aluminum by Ultrashort Laser Pulses Focused on a Tamped Target. Physical Review Letters, 1999, 82, 4843-4846.	7.8	184
3	Hot Dense Capsule-Implosion Cores Produced byZ-Pinch Dynamic Hohlraum Radiation. Physical Review Letters, 2004, 92, 085002.	7.8	105
4	Xâ€ray spectroscopy of highâ€energy density inertial confinement fusion plasmas. Physics of Fluids B, 1993, 5, 3328-3336.	1.7	69
5	ZAPP: The Z Astrophysical Plasma Properties collaboration. Physics of Plasmas, 2014, 21, .	1.9	63
6	Escape factors for Stark-broadened line profiles. Journal of Physics B: Atomic and Molecular Physics, 1987, 20, 2975-2987.	1.6	60
7	Dynamic hohlraum radiation hydrodynamics. Physics of Plasmas, 2006, 13, 056301.	1.9	60
8	Effects of ion dynamics and opacity on Stark-broadened argon line profiles. Physical Review E, 1996, 53, 1042-1050.	2.1	58
9	Modeling of population kinetics of plasmas that are not in local thermodynamic equilibrium, using a versatile collisional-radiative model based on analytical rates. Physical Review E, 2009, 80, 056402.	2.1	56
10	lon Dynamics Effect on Stark-Broadened Line Shapes: A Cross-Comparison of Various Models. Atoms, 2014, 2, 299-318.	1.6	44
11	Time-resolved spectroscopic measurements of high density in Ar-filled microballoon implosions. Physical Review Letters, 1989, 63, 267-270.	7.8	43
12	Multispectral x-ray imaging with a pinhole array and a flat Bragg mirror. Review of Scientific Instruments, 2005, 76, 073708.	1.3	42
13	Accretion disk dynamics, photoionized plasmas, and stellar opacities. Physics of Plasmas, 2009, 16, 041001.	1.9	41
14	Theoretical and experimental studies of laser-produced plasmas driven by high-intensity femtosecond laser pulses. Physics of Plasmas, 1997, 4, 1811-1817.	1.9	33
15	Dopant radiative cooling effects in indirect-drive Ar-doped capsule implosion experiments. Physical Review E, 2005, 72, 066403.	2.1	30
16	Laser absorption, mass ablation rate, and shock heating in direct-drive inertial confinement fusion. Physics of Plasmas, 2007, 14, 056305.	1.9	30
17	Processing of multi-monochromatic x-ray images from indirect drive implosions at OMEGA. Review of Scientific Instruments, 2003, 74, 1951-1953.	1.3	29
18	Benchmark Experiment for Photoionized Plasma Emission from Accretion-Powered X-Ray Sources. Physical Review Letters, 2017, 119, 075001.	7.8	29

#	Article	IF	CITATIONS
19	Spectroscopic determination of temperature and density spatial profiles and mix in indirect-drive implosion cores. Physical Review E, 2007, 76, 056403.	2.1	28
20	Absorption spectroscopy of a laboratory photoionized plasma experiment at Z. Physics of Plasmas, 2014, 21, .	1.9	27
21	Investigation of a polychromatic tomography method for the extraction of the three-dimensional spatial structure of implosion core plasmas. Physics of Plasmas, 2012, 19, 082705.	1.9	25
22	Direct asymmetry measurement of temperature and density spatial distributions in inertial confinement fusion plasmas from pinhole space-resolved spectra. Physics of Plasmas, 2014, 21, .	1.9	25
23	Observation of early shell-dopant mix in OMEGA direct-drive implosions and comparisons with radiation-hydrodynamic simulations. Physics of Plasmas, 2014, 21, .	1.9	25
24	Measurements of core and compressed-shell temperature and density conditions in thick-wall target implosions at the OMEGA laser facility. Physical Review E, 2011, 83, 066408.	2.1	23
25	Control and diagnosis of temperature, density, and uniformity in x-ray heated iron/magnesium samples for opacity measurements. Physics of Plasmas, 2014, 21, .	1.9	23
26	The dense Z-pinch program at the University of Nevada, Reno. , 1997, , .		22
27	Systematic Fuel Cavity Asymmetries in Directly Driven Inertial Confinement Fusion Implosions. Physical Review Letters, 2017, 118, 135001.	7.8	22
28	Processing of spectrally resolved x-ray images of inertial confinement fusion implosion cores recorded with multimonochromatic x-ray imagers. Journal of Applied Physics, 2011, 109, .	2.5	21
29	Observation of interspecies ion separation in inertial-confinement-fusion implosions. Europhysics Letters, 2016, 115, 65001.	2.0	21
30	Comparison of genetic-algorithm and emissivity-ratio analyses of image data from OMEGA implosion cores. Review of Scientific Instruments, 2008, 79, 10E921.	1.3	20
31	Analysis of time-resolved argon line spectra from OMEGA direct-drive implosions. Review of Scientific Instruments, 2008, 79, 10E310.	1.3	20
32	Application of fall-line mix models to understand degraded yield. Physics of Plasmas, 2008, 15, .	1.9	18
33	Al   1 s - 2 p absorption spectroscopy of shock-wave heating and compression in laser-driven planar foil. Physics of Plasmas, 2009, 16, .	1.9	18
34	Kinetic effects and nonlinear heating in intense x-ray-laser-produced carbon plasmas. Physical Review E, 2014, 90, 051102.	2.1	18
35	Multispectral x-ray imaging for core temperature and density maps retrieval in direct drive implosions. Review of Scientific Instruments, 2006, 77, 10E303.	1.3	17
36	Development of two mix model postprocessors for the investigation of shell mix in indirect drive implosion cores. Physics of Plasmas, 2007, 14, 072705.	1.9	17

#	Article	IF	CITATIONS
37	Laboratory measurements of resistivity in warm dense plasmas relevant to the microphysics of brown dwarfs. Nature Communications, 2015, 6, 8742.	12.8	17
38	Kinetic modeling of x-ray laser-driven solid Al plasmas via particle-in-cell simulation. Physical Review E, 2017, 95, 063203.	2.1	17
39	Observation and modeling of interspecies ion separation in inertial confinement fusion implosions via imaging x-ray spectroscopy. Physics of Plasmas, 2017, 24, 056305.	1.9	15
40	Spectroscopic analysis of Arâ€doped laserâ€driven implosions. Review of Scientific Instruments, 1995, 66, 755-757.	1.3	14
41	Multispectral imaging of continuum emission for determination of temperature and density profiles inside implosion plasmas. Journal of Quantitative Spectroscopy and Radiative Transfer, 2004, 88, 433-445.	2.3	14
42	Compressed shell conditions extracted from spectroscopic analysis of Ti K-shell absorption spectra with evaluation of line self-emission. Physics of Plasmas, 2014, 21, .	1.9	13
43	Reconstruction of quasimonochromatic images for multispectral x-ray imaging with a pinhole array and a flat Bragg mirror. Review of Scientific Instruments, 2006, 77, 083504.	1.3	12
44	Time-resolved characterization and energy balance analysis of implosion core in shock-ignition experiments at OMEGA. Physics of Plasmas, 2014, 21, .	1.9	12
45	Study of laser produced plasma in a longitudinal magnetic field. Physics of Plasmas, 2019, 26, .	1.9	12
46	Magnetic field impact on the laser heating in MagLIF. Physics of Plasmas, 2020, 27, .	1.9	12
47	Spectroscopic modeling of an argon-doped shock-ignition implosion. Review of Scientific Instruments, 2010, 81, 10E307.	1.3	9
48	Shell stability and conditions analyzed using a new method of extracting shell areal density maps from spectrally resolved images of direct-drive inertial confinement fusion implosions. Physics of Plasmas, 2016, 23, .	1.9	9
49	X-ray heating and electron temperature of laboratory photoionized plasmas. Physical Review E, 2020, 101, 051201.	2.1	9
50	Modelling, design and diagnostics for a photoionised plasmaÂexperiment. Astrophysics and Space Science, 2009, 322, 117-121.	1.4	8
51	Temperature distributions and gradients in laser-heated plasmas relevant to magnetized liner inertial fusion. Physical Review E, 2020, 102, 023209.	2.1	8
52	Multiobjective method for fitting pinhole image intensity profiles of implosion cores driven by a Pareto genetic algorithm. Review of Scientific Instruments, 2006, 77, 10F525.	1.3	7
53	Spatial structure analysis of direct-drive implosion cores at OMEGA using x-ray narrow-band core images. Review of Scientific Instruments, 2006, 77, 10E320.	1.3	7
54	Progress on observations of interspecies ion separation in inertial-confinement-fusion implosions via imaging x-ray spectroscopy. Physics of Plasmas, 2019, 26, 062702.	1.9	7

#	Article	IF	CITATIONS
55	Solid-Density Ion Temperature from Redshifted and Double-Peaked Stark Line Shapes. Physical Review Letters, 2021, 127, 205001.	7.8	6
56	Radiation hydrodynamic simulation of a photoionised plasma experiment at the Z facility. Astrophysics and Space Science, 2011, 336, 189-194.	1.4	5
57	Multiple-view spectrally resolved x-ray imaging observations of polar-direct-drive implosions on OMEGA. Physics of Plasmas, 2014, 21, 122704.	1.9	5
58	Understanding reliability and some limitations of the images and spectra reconstructed from a multi-monochromatic x-ray imager. Review of Scientific Instruments, 2015, 86, 113505.	1.3	5
59	Narrow-band x-ray imaging for core temperature and density maps retrieval of direct drive implosions. , 2006, , .		4
60	Assessment of transient effects on the x-ray spectroscopy of implosion cores at OMEGA. Journal of Physics B: Atomic, Molecular and Optical Physics, 2015, 48, 224006.	1.5	4
61	Spectroscopy of plasmas at solid density generated by ultra-short laser pulses. AIP Conference Proceedings, 2000, , .	0.4	3
62	X-Ray Spectroscopy of Dense Plasmas Produced by Isochoric Heating with Ultrashort Laser Pulses. AIP Conference Proceedings, 2004, , .	0.4	3
63	Observation of ionization trends in a laboratory photoionized plasma experiment at Z. Physical Review E, 2021, 104, 035202.	2.1	3
64	Investigating radiatively driven, magnetized plasmas with a university scale pulsed-power generator. Physics of Plasmas, 2022, 29, 042107.	1.9	3
65	Core Temperature and Density Gradients in ICF. AIP Conference Proceedings, 2004, , .	0.4	2
66	Data processing of absorption spectra from photoionized plasma experiments at Z. Review of Scientific Instruments, 2010, 81, 10E324.	1.3	2
67	The design of a photoionization front experiment using the Z-Machine as a driving source and estimated measurements. Physics of Plasmas, 2021, 28, .	1.9	2
68	MULTI-OBJECTIVE SPECTROSCOPIC DATA ANALYSIS OF INERTIAL CONFINEMENT FUSION IMPLOSION CORES: PLASMA GRADIENT DETERMINATION. Advances in Natural Computation, 2004, , 341-364.	0.1	2
69	Impact of 3D effects on the characteristics of a multi-monochromatic x-ray imager. Applied Optics, 2019, 58, 4753.	1.8	2
70	Development and integration of photonic Doppler velocimetry as a diagnostic for radiation driven experiments on the Z-machine. Review of Scientific Instruments, 2022, 93, 043502.	1.3	2
71	Spectroscopic Determination of Gradients in Indirect-Drive OMEGA Implosion Cores. AIP Conference Proceedings, 2002, , .	0.4	1
72	Spectroscopic Determination of Core Gradients in Inertial Confinement Fusion Implosions. AIP Conference Proceedings, 2002, , .	0.4	1

ROBERTO C MANCINI

#	Article	IF	Citations
73	Line Broadening Analysis of Argon X-Ray Emission from Z-Driven Implosions Cores. AIP Conference Proceedings, 2006, , .	0.4	1
74	Four-objective analysis including an optically thick line to extract electron temperature and density profiles in ICF implosion cores. Journal of Physics: Conference Series, 2008, 112, 022014.	0.4	1
75	Development of a spectroscopic technique for simultaneous magnetic field, electron density, and temperature measurements in ICF-relevant plasmas. Review of Scientific Instruments, 2016, 87, 11E558.	1.3	1
76	Stark-Broadening of Ar K-Shell Lines: A Comparison between Molecular Dynamics Simulations and MERL Results. Atoms, 2021, 9, 9.	1.6	1
77	Self-radiography of imploded shells on OMEGA based on additive-free multi-monochromatic continuum spectral analysis. Physics of Plasmas, 2020, 27, .	1.9	1
78	Diagnostic of energetic electrons in dense z-pinch plasmas. , 1997, , .		0
79	Spectroscopic study of temperature and density spatial profiles and mix in implosion cores. , 2008, , .		0
80	Characterizing the Effect of Magnetization at >10 KT in Cylindrically Imploded Hot Dense Plasmas Using Dopant Spectroscopy Techniques and Benchmarked Simulations. , 2022, , .		0